Available online at www.sciencedirect.com
SCIENCE DIRECT®
Diamond & Related Materials 14 (2005) 1770 – 1775
DIAMOND AND RELATED MATERIALS
www.elsevier.com/locate/diamond

Microwave plasma chemical vapor deposition of cone-like structure of diamond/SiC/Si on Si (100)

Jhih-Kun Yan *, Li Chang

Department of Materials Science and Engineering, National Chiao Tung University, 1001 Ta Hsueh Rood, Hsinchu, Taiwan 300, ROC

Available online 17 October 2005

Abstract

Diamond deposition on 1×1 cm^2 Si (100) substrates with bias was carried out by microwave plasma chemical vapor deposition (MPCVD). Distribution of deposited diamonds has been significantly improved in uniformity over all the Si substrate surface area by using a novel designed dome-shaped Mo anode. The deposits were characterized by scanning electron microscopy (SEM), transmission electron microscopy (TEM), and Raman analysis. SEM observations show that there is a high density of cone-like particles uniformly deposited on the surface of the substrate in short bias nucleation period. The average diameter, height and density of cone-like structure were increased with methane concentration in the bias stage. TEM reveals that the cone-like structure is actually composed of Si conic crystal covered with diamond. Between Si and diamond, a thin layer of cubic SiC is found in epitaxy with Si. Furthermore, for 3% CH_4 concentration, the range of diameter of cone-like structure was about 20–90 nm and the size of diamond was about 10–60 nm.

Keywords: Diamond; Nucleation; Epitaxy; Transmission electron microscopy (TEM)

1. Introduction

In CVD processes for the nucleation of diamond on silicon substrates, the bias-enhanced nucleation (BEN) has been a widely used method because it can increase the nucleation density on mirror-polished silicon [1,2] and supply nuclei for the growth of heteroepitaxial layers [3]. The BEN process consisting of the superposition of a microwave plasma with a modified dc glow discharge has been extensively studied [4–8]. Stöckel et al. [8] have shown the spatiotemporal evolution of the dc glow discharge according to the formed diamond nuclei moving from the edge to the sample center. As a result, uniform deposition of diamond is difficult to be obtained by the BEN method. Stoner et al. [2] reported the formation of an interfacial layer of β-SiC and amorphous carbon has been observed during the BEN step. The result has led to a conclusion that β-SiC layer may be helpful for diamond nucleation on Si due to the reduced mismatch between diamond and Si. Although the mechanisms of BEN process have been studied [9–12], the processes leading to the nucleation have not yet been fully understood. One of the reasons for the difficulty of the nucleation and growth study may be due to uneven spatial distribution of diamond nuclei in terms of size, shape, density, and interface [13], in addition to the temporal BEN process in bias time and CH_4 concentration.

In this work, to facilitate the understanding of the mechanisms during the bias step without the spatial variation of diamond deposition in radial direction on the substrate, we have designed a Mo anode to improve the distribution of microwave plasma and dc glow discharge which has succeeded to obtain uniform diamond deposits on Si substrate. As a result, uniform cone-like structures can be deposited in short bias time. Also, the effect of CH_4 concentration is evaluated based on the results of Raman spectroscopy and electron microscopy. In particular, the constituents of cone-like structure were investigated.

2. Experimental

The nucleation of diamond was carried out in a 2.45-GHz ASTeX microwave plasma CVD reactor. In order to optimize the microwave discharge and the extension of the bias discharge over the whole substrate, we designed a dome-

* Corresponding author. Tel.: +886 3 5712121x55373; fax: +886 3 5724727.
E-mail address: zhikun.mse91g@nctu.edu.tw (J.-K. Yan).

0925-9635/$ - see front matter © 2005 Elsevier B.V. All rights reserved.
doi:10.1016/j.diamond.2005.09.019

Table 1
Experimental deposition parameters for diamond nucleation

	Heating	Bias
Power (W)	800	500
Pressure (Torr)	20	20
CH_4 in H_2 (%)	2	3∼5
Bias voltage (V)	0	−100
Flow rate (sccm)	300	300
Duration (min)	10	2

shaped Mo anode with a diameter of 15 mm which was located above the substrate as counter-electrode. The distance between the anode and substrates was varied in the range from 15 to 30 mm. The substrate was mirror-polished *p*-type (100) silicon wafer with dimension of 1×1 cm^2 without any mechanical pretreatment. Before the experiment, the substrate was etched in 1% hydrofluoric acid concentration in de-ionized water for 60 s to remove native oxide of Si, and ultrasonically cleaned with acetone for 10 min. The substrate was then placed on a Mo disk holder. A hydrogen plasma with addition of 2% CH_4 concentration was initially applied to the substrate for 10 min for heating to the required temperature (about 800 °C) as measured by an optical pyrometer and to remove any residual of native oxide on the Si substrate surface, followed by applying a bias voltage of 100 V on the anode for 2 min with different methane concentration. The detailed process parameters are listed in Table 1. In particular, the growth step is not performed for the nucleation study. Samples obtained by biasing with 3%, 4% and 5% CH_4 are designated as A, B and C, respectively. After the bias process, the surface morphologies and microstructures were examined using a JEOL JSM-6330F field-emission scanning electron microscope (SEM) and a Philips Tecnai 20 transmission electron microscopy (TEM). Electron energy-loss spectroscopy (EELS) was performed using a Gatan Imaging Filter equipped with the TEM. An argon ion gas laser (wavelength 514.5 nm) with 20 mW power was employed for the acquisition of Raman spectra.

3. Results and discussion

The improvement of the distribution of microwave plasma and dc glow discharge using the dome-shaped Mo anode for bias is demonstrated by the morphologies observed at three different local areas on the substrate along the diagonal from corner to corner through the center, with a 4.5-mm distance between each location, are shown in Fig. 1(a), (b) and (c), respectively. (Deposition condition: Mo anode, bias −100 V (substrate), 4% CH_4/60 s and growth 0.667% CH_4/10 h.) It is apparent that the distribution of diamond is quite uniform in terms of the density, size and shape. The uniformity is also supported by micro-Raman spectra from different areas which all show the same result.

After the uniformity of diamond deposition was ensured, we then carried out the nucleation study without further growth. Fig. 2(a) shows the surface morphology of sample A after the bias stage using 3% CH_4 for 2 min. The nucleation density estimated from SEM is about 8×10^8 cm^{-2}. In Fig. 2(b), a high-magnification view of Fig. 2(a) shows that the deposited particles have a cone-like shape. The range of base diameter of cone-like particles was 20–90 nm, with the average of ∼40 nm. The image contrast of the cone-like particles shows that the top half is in bright contrast, whereas the bottom half is in dark. In fact, the top half bright regions are of diamond crystallinity as shown in the following TEM results. The diamond size is smaller, in the range of about 10–60 nm. With the increase of methane concentration, the nucleation density is increased to about 6×10^9 and 1×10^{10} cm^{-2} respectively, as estimated from Figs. 2(c) and (e) for samples B (4% CH_4) and C (5% CH_4). Similar cone-like particles can be observed in high-magnification images of Figs. 2(d) and (f) as well. Their sizes are also increased with methane concentration, as can be seen that the average base diameter of cone was about 55 nm and 75 nm, respectively, and their heights are also increased. It

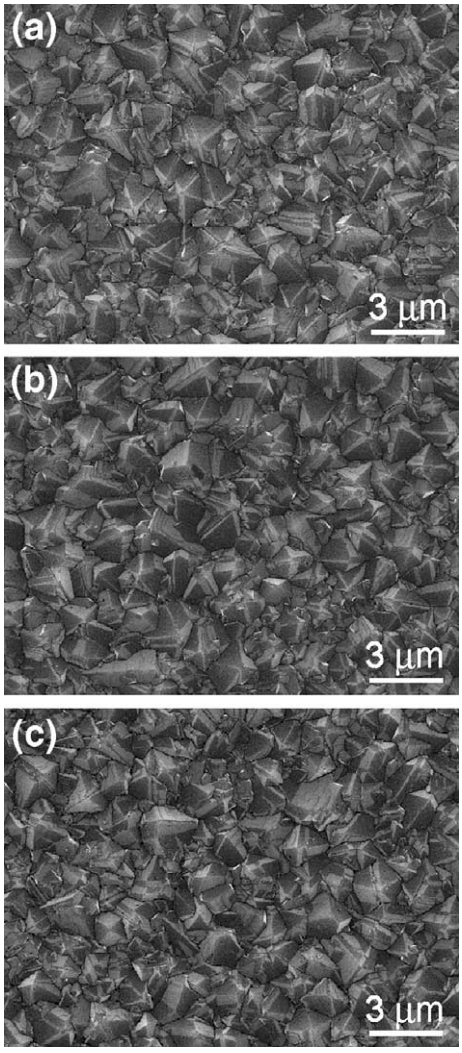

Fig. 1. SEM images of diamond film observed at three different local areas along the diagonal of the 1×1 cm^2 substrate from corner to corner through the center: (a) one corner, (b) center, and (c) another corner. The distance between each sampling location is about 4.5 mm. Deposition condition: Mo anode, bias −100 V (substrate), 4% CH_4/60 s and growth 0.667% CH_4/10 h. No mechanical pretreatment.

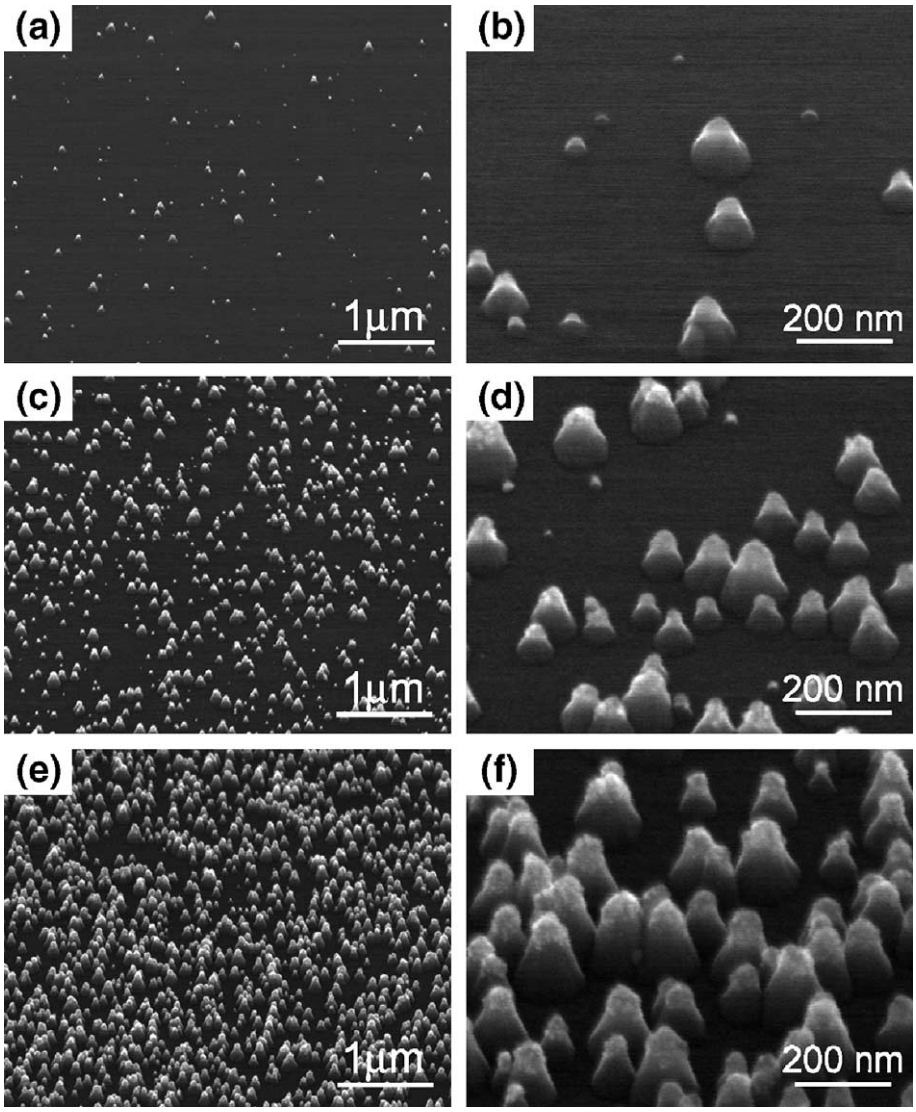

Fig. 2. SEM micrographs of the cone-like particles synthesized by the different CH_4 concentration: (a) Sample A with high magnification in (b); (c) Sample B with high magnification in (d); (e) Sample C with high magnification in (f).

is also noticed that sample C has a much more uniform size distribution with a high density of diamond particles.

The corresponding Raman spectra of samples A, B and C are presented in Fig. 3. For sample A, no peaks can be identified, while for samples B and C, the spectra clearly show two broad peaks at approximately 1340 cm^{-1} and 1585–1606 cm^{-1}. The broad 1340 cm^{-1} peak might result from the contribution of the 1332 cm^{-1} and 1350 cm^{-1} (D band). As the 1332 cm^{-1} is characteristic of crystalline diamond, it suggests that the diamond phase has indeed been deposited. The other band around 1585–1606 cm^{-1} (G band) is closely related to characteristics of disordered sp^2-bonded arrangements which normally give rise to the D band around 1350 cm^{-1} as well [14,15]. This shows that a significant amount of non-diamond species is formed in the early stage of deposition.

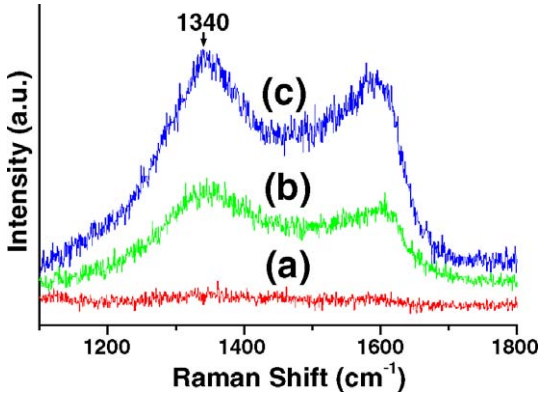

Fig. 3. Raman spectra from (a) Sample A, (b) Sample B, and (c) Sample C.

The bright-field TEM micrograph in Fig. 4(a) shows the cross-sectional view of the interfacial region between the cone-like particles and Si substrate from sample A. The image contrast of the particles is seen to consist of two distinctive regions: one is on the top-half in bright contrast and the other is on the bottom in darkness, similar to the SEM observation in Fig. 2. The bottom-dark cone in triangular shape is apparent of single-crystalline Si, which is ~20 nm in height and ~60 nm

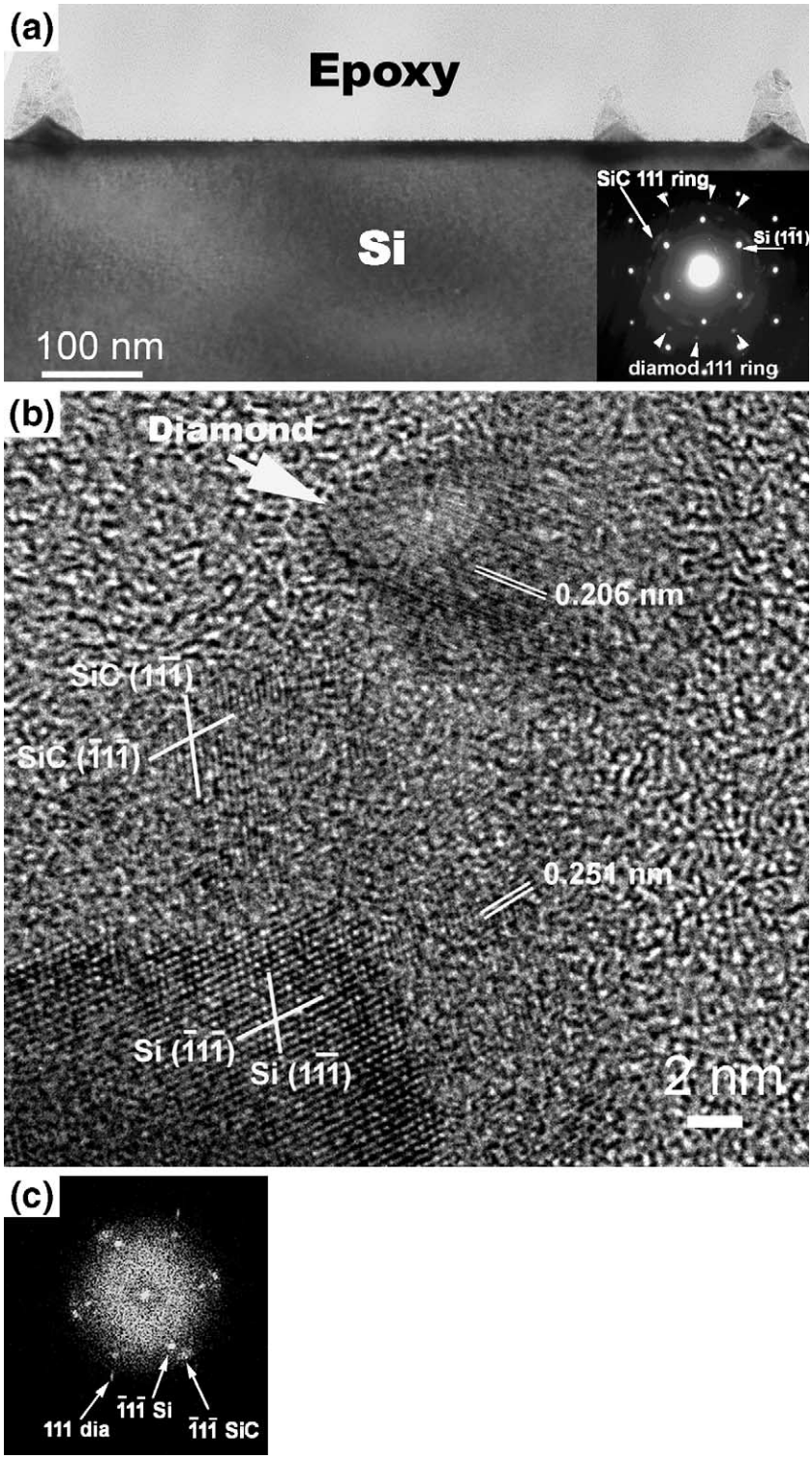

Fig. 4. Cross-sectional TEM showing the cone-structure on Si (100) substrate from Sample A; (a) bright-field image with the inset of the corresponding selected area diffraction pattern in Si [011] zone axis; (b) HRTEM image of cone-like structure from another area in the same TEM specimen, and (c) FFT image of (b).

in diameter. Both sides have equal length and are perpendicular to Si <111>. The interface is smooth, and the surface of the substrate between the cones is also flat, implying that the bias at −100 V has resulted in negligible damage on the Si. The reason for the formation of Si cone is not understood at the moment; thus, further study is needed. The inset in Fig. 4(a) is the corresponding electron diffraction pattern along Si [011] zone-axis in which diamond and cubic SiC {111} rings can be identified. As the image contrast in Fig. 4(a) does not show the difference between SiC and diamond, we further characterize the microstructure using high-resolution TEM (HRTEM) and EELS mapping. Fig. 4(b) shows a HRTEM image of a cone-like structure from another area in the same TEM specimen. Both lattice fringes of SiC {111} (spacing of 0.25 nm) and

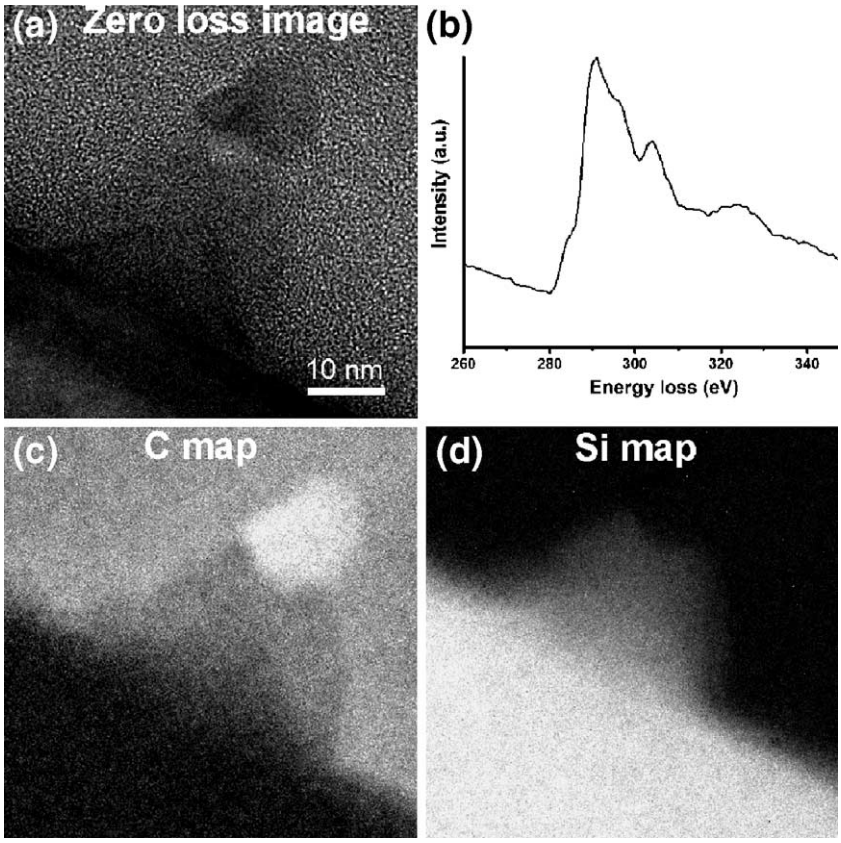

Fig. 5. (a) Zero loss image of cone-like structure from sample A; (b) EELS spectrum from diamond showing carbon K edge; (c) carbon map; and (d) silicon map.

diamond {111} (spacing of 0.206 nm) can be clearly seen. Fig. 4(c) is a fast-Fourier-transformed (FFT) pattern of Fig. 4(b). It shows the existence of SiC in epitaxy with Si, while the diamond has no specific crystallographic relationship with SiC and Si as the lattice fringes are not parallel to those of Si and SiC.

The core loss signals of the carbon K edge (284 eV) and the silicon L edge (99 eV) in an energy window of 10 eV were used for elemental mapping. In Fig. 5(a), the same location with the HRTEM image in Fig 4(b) shows the zero loss image. Fig. 5(b) is the EELS spectrum obtained from the diamond particle on top of the cone, showing the diamond characteristics of carbon K-edge. Compared with the zero loss image, the Fig. 5(c) shows the carbon distribution in which the brightest area is corresponding to the diamond region. Besides the diamond area, other less bright area between diamond and Si cone is SiC. The Si map in Fig. 5(d) shows that the brightest area is Si substrate and the darkest region is diamond. The contrast levels in both Si and C maps are complementary with each other, clearly showing the distribution of Si, SiC, and diamond phases. The Si cone is fully covered with SiC. The clearly identified diamond region may be a single particle as HRTEM shows only one set of the fringes. The SiC phase has a thickness of about 10 nm, and has a V-shape grooved region on the top where it is covered with the diamond, suggesting that it is the site for diamond nucleation. The nucleation of diamond at the grooved site has been observed also in TEM by Lee et al. [16].

From the above result, the cone-like structure is actually composed of Si crystal covered with diamond. Between Si and diamond, a thin layer of cubic SiC is found in epitaxy with Si. Similar TEM results have been observed for samples B and C (not shown).

4. Summary

The result shows that uniform diamond deposition can be obtained by short bias nucleation period using a dome-shaped Mo anode. After the deposition of diamond nucleation, observations of SEM and TEM show formation of cone-like structure consisting of a Si cone covered with epitaxial cubic SiC of a grooved shape which is topped with diamond. The average diameter, height and density of cone-like structure were increased with methane concentration in the bias stage.

Acknowledgements

This work was supported by National Science Council, Taiwan, ROC under contract of NSC 93-2216-E-009-014.

References

[1] S. Yugo, T. Kanai, T. Kimura, T. Muto, Appl. Phys. Lett. 58 (1991) 1036.
[2] B.R. Stoner, G.H. Ma, S.D. Wolter, J.T. Glass, Phys. Rev., B 45 (1992) 11067.

[3] X. Jiang, C.P. Klages, R. Zachai, M. Hartweg, H.J. Füsser, Appl. Phys. Lett. 62 (1993) 3438.
[4] I.-H. Choi, S. Barrat, E. Bauer-Grosse, Diamond Relat. Mater. 12 (2003) 361.
[5] S. Barrat, S. Saada, I. Dieguez, E. Bauer-Grosse, J. Appl. Phys. 84 (1998) 1870.
[6] M. Schreck, T. Baur, B. Stritzker, Diamond Relat. Mater. 4 (1995) 553.
[7] W. Kulisch, L. Achermann, B. Sobisch, Phys. Status Solidi A 154 (1996) 155.
[8] R. Stöckel, K. Janischowsky, S. Rohmfeld, J. Ristein, M. Hundhausen, L. Ley, Diamond Relat. Mater. 5 (1996) 321.
[9] S. Yugo, T. Kimura, T. Kanai, Diamond Relat. Mater. 2 (1992) 328.
[10] S.P. McGinnis, M.A. Kelly, S.B. Hagstrom, Appl. Phys. Lett. 66 (1995) 3117.
[11] J. Roberson, J. Gerber, S. Sattel, M. Weiler, K. Lung, H. Ehrhardt, Appl. Phys. Lett. 66 (1995) 3287.
[12] P. Wurzinger, P. Pongratz, J. Gerber, H. Ehrhardt, Diamond Relat. Mater. 5 (1996) 345.
[13] C.J. Chen, L. Chang, T.S. Lin, F.R. Chen, J. Mater. Res. 10 (1995) 3041.
[14] V. Mennella, G. Monaco, L. Colangeli, E. Bussoletti, Carbon 33 (1995) 115.
[15] A.C. Ferrari, J. Robertson, Phys. Rev., B. 61 (2000) 14095.
[16] S.T. Lee, H.Y. Peng, X.T. Zhou, N. Wang, C.S. Lee, I. Bello, Y. Lifshitz, Science 287 (2000) 104.